

## Forced Convective Heat Transfer and Pressure Drop of Air Flowing in a Rectangle Duct with Cross-Ribs on the Opposite Walls

B. Deng<sup>1</sup>    T. T. Wong<sup>2</sup>    W. Q. Tao<sup>1</sup>

1. School of Power and Energy, Xi'an Jiaotong University, Xi'an, Shaanxi, China

2. Department of Mechanical Engineering, The Hong Kong Polytechnic University, Hung Hom, Kowloon, Hong Kong, Email: wqtao@mail.xjtu.edu.cn

Experiments were conducted to investigate the forced convective heat transfer and flow friction of turbulent airflow in a rectangular duct with cross-ribs attached at the two principal walls in the Reynolds number range from 5000 to 40000. The effect of the rib cross angle (45°, 60°, 75°) and the height (4 mm, 5 mm) of the cross-ribs on the forced convection and flow friction were tested. Non-dimensional correlations for the duct average Nusselt number and friction factor of cross-ribs duct were developed from the test data. Experiments were also conducted for the corresponding parallel ribs to compare their relative performance. The experimental results show that both of the convective heat transfer coefficient and friction factor were increased with cross-ribs, with 45° cross-ribs being the best. Compared with parallel ribs normal to the flow direction under identical flow rate and identical pumping power constraints, the cross-ribs can enhance heat transfer in the lower Reynolds number region, while in the high Reynolds number region, the heat transfer performance of the parallel ribs seems better.

**Keywords:** cross-ribs, forced convection, heat transfer enhancement.

### Introduction

Artificial roughness on a surface has been widely accepted as an effective technique to enhance the heat transfer rate in a heat exchanger or a cooling passage of gas turbine blade. Roughness elements are used to improve the convective heat transfer by creating turbulence in the flow, however, it also results in an increase in pressure losses and greater fan or blower is required. In order to keep the pressure losses at a minimum level, the turbulence must be created only in the region very close to the duct surface, i.e. in laminar sublayer. Usually, the roughness elements were small ridges of a square cross section and were placed periodically at right angle to the main flow direction. The cost paid for the higher heat transfer was an increase in the pressure drop. A number of investigations have been carried out on the heat transfer characteristics of rectangular ducts with small ribs placed at right angle to the main flow direction, and only those works published in the nineties will be briefly reviewed. Lau and Han<sup>[1,2]</sup>

investigated experimentally the heat transfer performance in straight channels with parallel, crossed, V-shaped and discrete rib turbulators. Liou and Hwang<sup>[3]</sup> investigated experimentally the turbulent heat transfer and friction in a channel with triangular, semicircular and square ribs on the walls. Lorenz et al. measured the distributions of heat transfer coefficient and pressure drop along the wall of a ribbed channel by means of infrared thermograph<sup>[4]</sup>. Hwashida studied experimentally the local heat transfer of ribbed surface with air of atmospheric pressure and room temperature as the working fluid<sup>[5]</sup>. Hwang and Liou<sup>[6]</sup> investigated experimentally the heat transfer performance of the slit-ribbed channel and compared its performance with that of the solid-ribbed channel. Saini and Saini<sup>[7]</sup> investigated the effect of expanded metal mesh as roughness element on the heat transfer coefficient and friction factor of a fully-developed turbulent flow in a rectangular duct with large aspect ratio. Chandra et al<sup>[8]</sup> carried out an investigation on the effect of circular and square rib profiles on turbulent channel flow heat

transfer and friction characteristics. Leung and Probert<sup>[9]</sup> investigated the forced convection of a turbulent flow of air in a horizontal, equilateral-triangular ducts. Wang et al. conducted study of developing turbulent flow and heat transfer in ribbed convergent square duct<sup>[10]</sup>.

The previous results were obtained primarily for parallel ribs on one or two principal walls of channels. A question may arise as whether the crossed ribs (the ribs on the one or two principal walls were cross-installed) can provided a better heat transfer performance than that of parallel ribs, and how the cross-rib angle and relative rib height affect heat transfer performance.

The objective of this experimental study is to investigate the effect of cross-ribs geometry on the heat transfer coefficient and friction factor in a rectangular duct having one or two principal walls artificially roughened by cross-ribs. Ribs of two different heights and three cross angles have been tested. Semi-empirical formulations for Nusselt number and friction factor in terms of Reynolds number for different roughness parameters have been developed. Performance comparison between the ducts with cross-ribs and parallel ribs have been made. The terminology "cross angle" used in this paper represents the angle composed of the axes of the two crossed-ribs. The so-called attack angle usually means the angle between the duct axis and the rib axis<sup>[1,2]</sup>. The three cross angles studied in this paper, 45°, 60° and 75°, correspond to three attack angles in positive and negative directions:  $\pm 22.5^\circ$ ,  $\pm 30^\circ$ ,  $\pm 37.5^\circ$ .

## Experimental Arrangement

### Test apparatus

In the present study, a rectangular duct was used to

simulate the fluid flow passage of a heat exchanger. The test apparatus consists of an entrance section (700 mm long), a test section (1000 mm long), a combination section (400 mm long), and an exit section (1400 mm long) (See Fig.1). The first three sections were fabricated with 18 mm wooden plate, having identical cross-sectional shape and dimensions (i.e. 150 mm wide, 30 mm high). They were joined together by using two flanges. The flange was made use of zinc sheet, wood and rubber. The wood and rubber were used as an insulator to avoid the end heat loss to the entrance and exit section from the test duct. A centrifugal blower driven by a 1.5 kW electric motor withdrew air through the flow loop. The air mass rate flow through the flow loop was controlled by an air adjust valve. A FC501 micromanometer, two thermocouple scanners, a Pitot tube are the major measuring instruments for air mass flow rate and temperature difference.

The details of the test duct is now addressed. A cross-sectional view of the test section is shown in Fig.2. As can be seen there, the top and bottom walls of the test duct consists of three layers, with a heating layer of 2 mm thick being sandwiched in between. Duralumin plates with 2 mm thick were adopted in this experiment because of its high conductivity and machinability. The ribs, also made from duralumin, were attached to the duralumin plate periodically with a thin layer of thermofoil (about 0.18 mm of average thickness) to ensure good contact. The lay-out of the cross-ribs on the top and bottom walls is presented in Fig.3 for the case of 45° cross-angle. It should be noted that in this experiment the nominal length of the test duct was 1000 mm, however for ribs of different cross-angles, the effective length may be less than 1000 mm in order to place integral number of cross-ribs, and this fact should

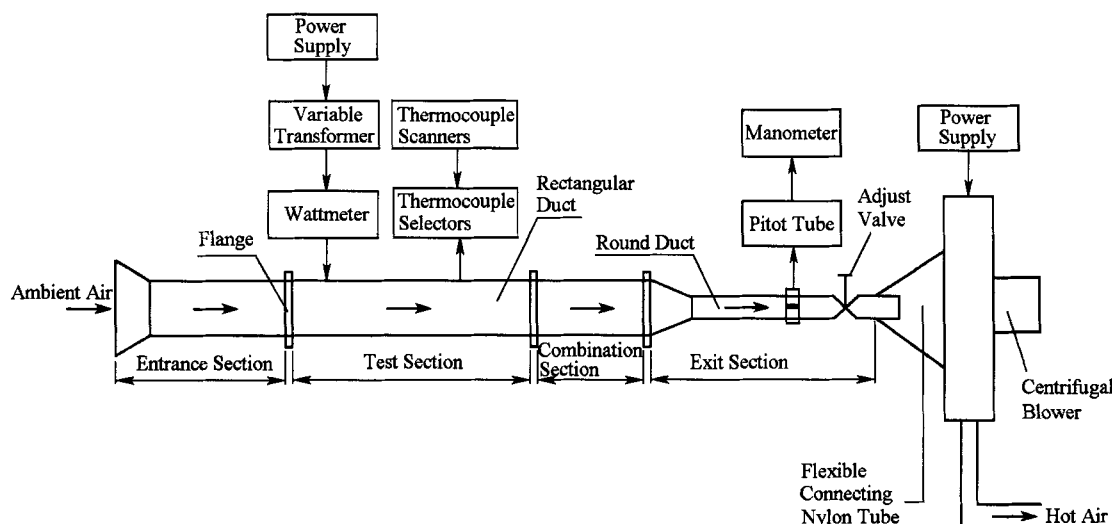


Fig.1 Experiment setup

be bear in mind when the total pressure drop across the entire enhanced section was to be measured.

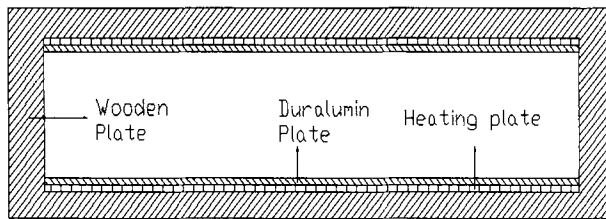


Fig.2 Cross-sectional view of the test section

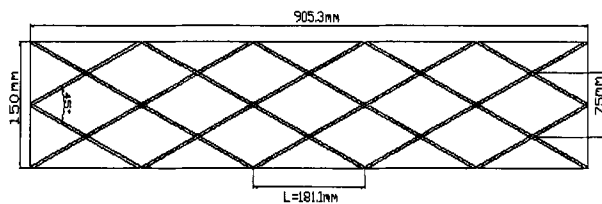


Fig.3 The arrangement of cross-ribs on the duralumin plate

The combination duct was designed to measure the exit temperatures accurately. In order to accurately measure the bulk temperature of heated fluid, special mixing devices were built in the combination duct. This device consists of two specially-fabricated plates positioned in the combination duct with a short distance in between (200 mm). The first plate has a centered big hole ( $200 \times 20 \text{ mm}^2$ ), while the second one possesses 8 small holes ( $\phi 14 \text{ mm}$ ) distributed in the plate (Fig.4). When air stream flowing through such two specially fabricated plates, strong mixing will occur, leading to a quite uniform temperature of the exit flow. The importance of such mixing device in the measurement of exit fluid from a heat exchanger device was indicated in [11], and recently re-addressed in [12].



Fig.4 The configurations of the two plates in the combination section

Uniform heating was provided by means of two electrically heating plates, which were fixed at the top and bottom surfaces of test duct with connecting bolts. The heated plate can supply a power up to 1800 W. The power supplied was measured by a power-meter and regulated by a variable transformer.

The test duct and combination duct were surrounded by 40 mm thick glass fibre blanket to minimize the heat loss from these two sections. The thermal conductivity of the glass fibre was estimated to be about  $0.35 \text{ W/m} \cdot \text{K}$ .

### Measurement of temperature, pressure drop and flow rate

#### 1. The measurement of inlet and outlet temperature

The inlet temperature was measured by a single T-type thermocouple positioned in front of the entrance duct. The thermocouples for measuring the outlet temperature were placed on a metal mesh connected with the flange between the combination duct and the exit duct. The arrangement of thermocouples on the metal mesh is shown in Fig.5.

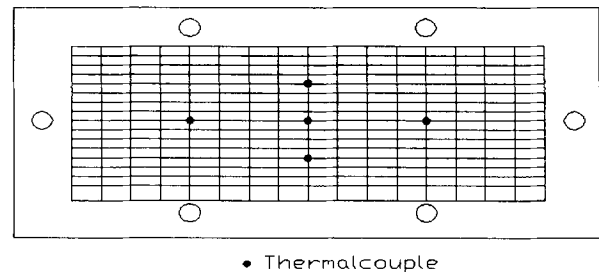


Fig.5 The thermocouples arrangement on the metal mesh

#### 2. The measurement of wall temperature

The wall temperatures of the test duct were also measured with T-type thermocouples. In each experiment the locations of the thermocouples were different, depending on the angle of cross-ribs on the duralumin plate. Taking the case of  $45^\circ$  cross angle as an example. The locations of thermocouples on the principal wall are shown in Fig.6. As shown there, in the center line of the duct five thermocouples were imbedded in the center of each parallelogram. To install the thermocouples, small holes and shallow grooves were machined on the backside of the duralumin plate. The grooves were 1 mm deep and 1 mm wide, being vertical to the axial centerline of duralumin plate. A small hole was drilled at the end of each shallow groove. The depth of each small hole was about 1mm. The details of the grooves and holes for the case of  $45^\circ$  cross angle are presented in Fig.7.

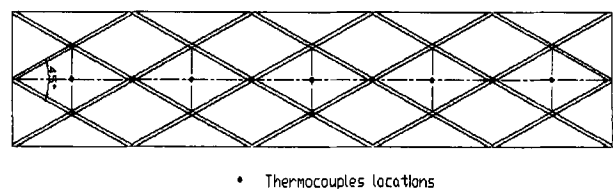


Fig.6 The thermocouples locations

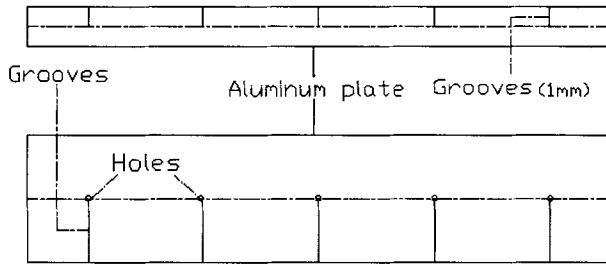


Fig.7 The thermocouple install locations on the backside of the duralumin plate

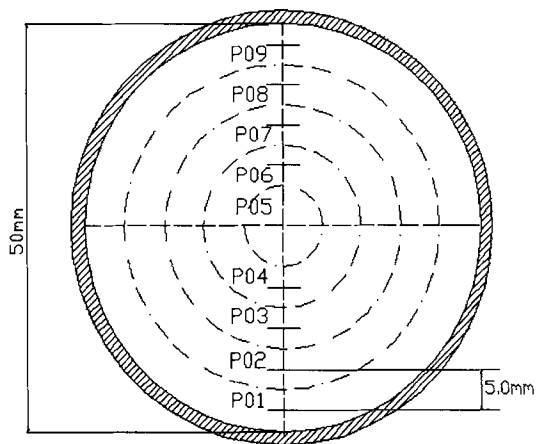
The junction of each thermocouples was then affixed to the small hole with the soldering tin and epoxy. Epoxy was also applied to the shallow groove to hold the thermocouples in place. Good physical contact between the thermocouple and the small grooves was checked with an Ohmmeter.

### 3. The measurement of pressure

In order to determine the axial pressure drop across the test section, two static pressure taps were installed in the center line of one of the side walls. The taps were fabricated with plexiglass. The diameter of the hole in the center of the pressure taps were 1.5 mm. An FC501 micromanometer was used to measure the pressure drop. It can measure pressure drop in the range of 2 Pa to 200 Pa with 1% error of reading.

### 4. The measurement of air flow rate

The air velocity distribution was measured through a Pitot tube<sup>[13]</sup>, which was fixed in the exit section with a diameter of 50 mm and equipped with a manometer. An adjust valve was installed at the inlet of the blower to control the air flow rate through the system (see Fig.1). The air velocity were taken from nine different locations



P01~P09: Nine Different Flow Velocity Measurement Point

Fig.8 Measurement locations of the air velocity distribution in the exit duct

with an interval of 5 mm across a cross section in the exit duct (Fig.8). Accurate positioning of the Pitot tube was achieved by using a vertical traversing mechanism mounted on a vernier caliper. The air flow rate was then obtained by numerical integration over the cross section.

## Data Reduction

The duct average Nusselt number and friction factor were defined as:

$$Nu = \frac{h_m De}{\lambda} \quad (1a)$$

$$f = \frac{(\Delta p / L) De}{(1/2) \rho u_m^2} \quad (1b)$$

where  $h_m$  is the duct average heat transfer coefficient,  $De$  is the equivalent diameter of the test section (50 mm), and  $\Delta p$  is the pressure drop over the test section within which the cross ribs were positioned.

The average heat transfer coefficient was determined by:

$$h_m = \frac{Q}{A(T_{w,m} - T_{f,m})} \quad (2)$$

where  $Q$  is the duct heat transfer rate,  $T_{w,m}$  is the average wall temperature and  $T_{f,m}$  is the average fluid temperature in the duct. During the experiment, thermal balance was made for each test run. It was required that the difference between the electric power input and the enthalpy increase of air was not larger than 5% of their average value and the air enthalpy increase was taken as the heat transfer rate. In the data reduction, the air thermal physical properties were taken from [14].

The dimensionless parameters used to describe the convection from the horizontal rectangular duct to the air flow were related by the following equation:

$$Nu = C_1 Re^m Pr^n \quad (3)$$

where constants  $C_1$ ,  $m$  and  $n$  should be determined by experimental data.

Throughout the temperature range studied, the Prandtl number ( $Pr$ ) of air remained almost constant ( $\sim 0.707$ ), therefore Equation (3) can be simplified to:

$$Nu_D = C_2 Re_D^m \quad (4)$$

Moreover, an empirical relation for friction factor in turbulent flow through a channel may be expressed as a power-law form:

$$f = C_3 Re_D^n \quad (5)$$

where constant  $C_3$  and  $n$  also should be determined by test data.

The values of  $C_2$ ,  $C_3$ ,  $m$  and  $n$  of Equation (3) and (4) obtained from least square method are listed in Table 1.

## Experimental Results

The duct averaged Nusselt number and friction factor are now presented. The test data consist of two groups. In one group (A-1), the top and bottom walls were both heated with cross-ribs installed only on one principal wall and the opposite wall was smooth. In the other group (A-2), both the top and bottom walls were roughened by the cross-ribs. In addition, for comparison purpose, experiments were also performed for ducts having parallel ribs with  $90^\circ$  of attack angle. For comparison purpose, the pitch of the parallel ribs equals to the axial diagonal of the cross ribs compared. For example, the referenced parallel ribs for the cross ribs of  $45^\circ$  takes the axial diagonal of this cross rib as its pitch. All these data were collected in group B.

### A-1. Two opposite walls were heated, the cross-ribs were positioned only on one wall

The cross-ribs include two heights (4 mm, 5 mm), and three angles ( $45^\circ$ ,  $60^\circ$  and  $75^\circ$ ). The final experimental results (including the heat transfer and friction factor) are presented in Fig.9(a)~Fig.9(f). The dashed lines shown in these figures are Dittus-Boelter equation or Blasius equation.

From these figures, following features may be noted: (1) For the cross-rib of same height, the larger the cross angle, the larger the duct average Nusselt number and

friction factor, with the variation from  $45^\circ$  to  $60^\circ$  being more significant. (2) For the same cross angle, the rib of 5 mm has a higher heat transfer coefficient with a greater pressure drop penalty.

### A-2. Two opposite walls were both heated and roughened

The experimental results are shown in Fig.10(a)~Fig.10(f), where again the dashed lines represents the Dittus-Boelter equation or Blasius equation. The variation trends of heat transfer coefficient and friction factor are obviously the same as the previous case and will not be restated here.

## B. Parallel-ribs installed

In order to compare the heat transfer performance of the cross-rib duct with the parallel-rib duct, experiments were also conducted for parallel-rib duct for the case of  $45^\circ$  cross angle (see Fig.3). The corresponding parallel rib arrangement is presented in Fig.11, where the thermocouple locations are also shown. Experiments were conducted for two cases: A — Two walls heated, one wall roughened; B — Two walls heated and roughened. The final experimental results of the parallel ribs are presented in Fig.12(a)~Fig.12(h).

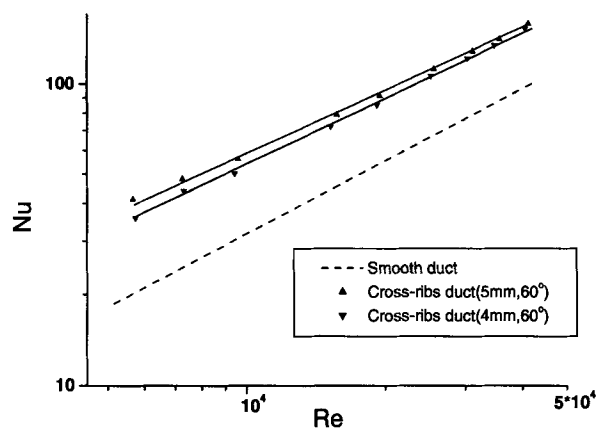
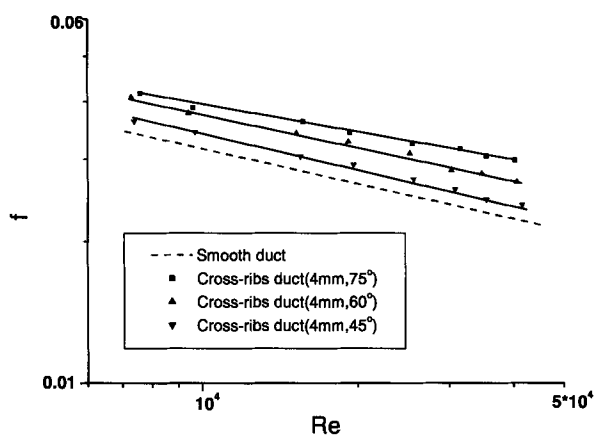
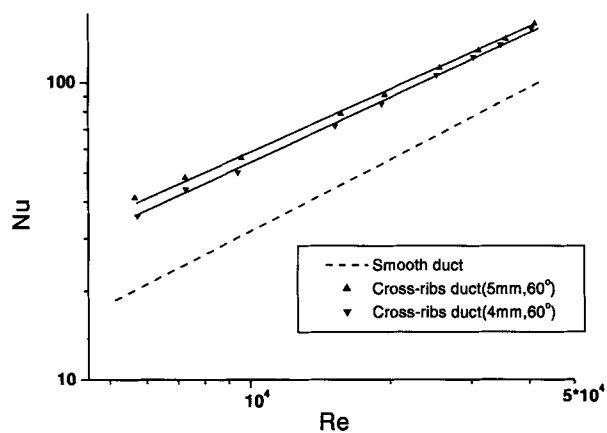
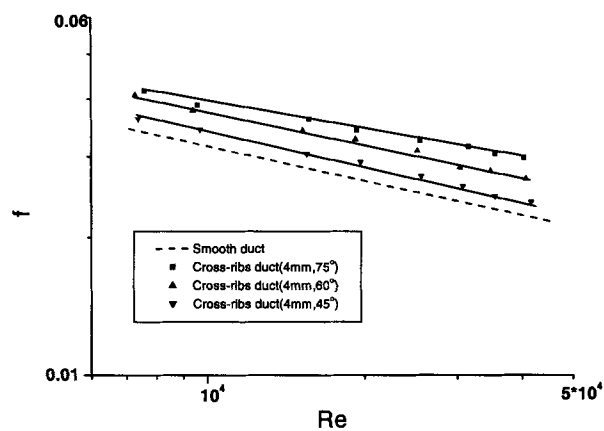
From these figures it can be stated that compared with the parallel rib, the cross-rib can enhance heat transfer with much greater pressure drop penalty.

## Performance Evaluation

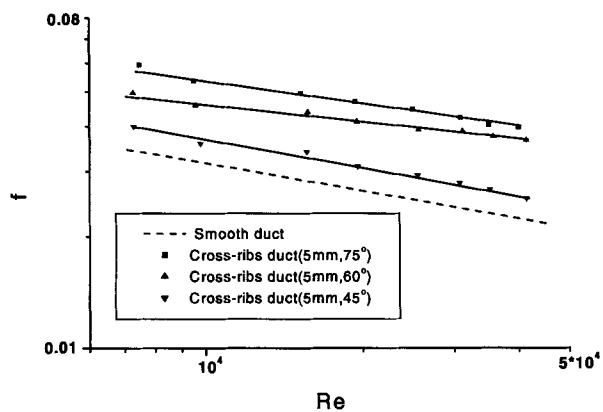
In comparing the performance of different types of ribs, it is necessary to specify the constraints under Which the comparisons is made<sup>[13]</sup>. There is a broad

Table 1 The parameters of equation (4), (5)

|          |              | Group A-1 |         |         |         |         |         | Group A-2 |         |         |         |        |        |
|----------|--------------|-----------|---------|---------|---------|---------|---------|-----------|---------|---------|---------|--------|--------|
|          |              | 4 mm      |         |         | 5 mm    |         |         | 4 mm      |         |         | 5 mm    |        |        |
|          |              | 45°       | 60°     | 75°     | 45°     | 60°     | 75°     | 45°       | 60°     | 75°     | 45°     | 60°    | 75°    |
| $Nu_D =$ | $C_2$        | 0.0361    | 0.0424  | 0.0691  | 0.0395  | 0.0706  | 0.0772  | 0.0608    | 0.0858  | 0.0835  | 0.0864  | 0.0867 | 0.0841 |
|          | $C_1 Re_D^m$ | $m$       | 0.7747  | 0.7663  | 0.7208  | 0.7696  | 0.7194  | 0.7129    | 0.7521  | 0.7321  | 0.7466  | 0.7244 | 0.7416 |
| $f =$    | $C_3$        | 0.7219    | 0.4825  | 0.5962  | 0.5196  | 0.3509  | 0.5027  | 0.5962    | 0.2468  | 0.3230  | 0.1112  | 0.3553 | 0.5560 |
|          | $C_2 Re_D^n$ | $n$       | -0.3151 | -0.2297 | -0.2443 | -0.2673 | -0.1917 | -0.1991   | -0.2443 | -0.0989 | -0.0908 | -0.048 | -0.098 |

(a) Average  $Nu$  of 4mm-rib duct(b) Average  $Nu$  of 5mm-rib duct(c)  $Nu$  comparison between 4mm and 5mm ribs

(d) Duct friction factor of 4mm-rib duct



(e) Duct friction factor of 5 mm-rib duct

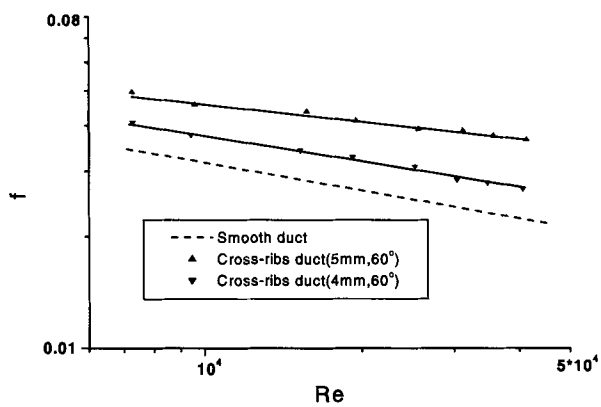
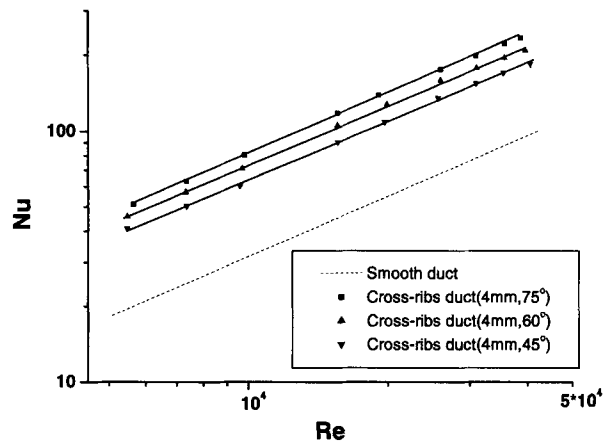
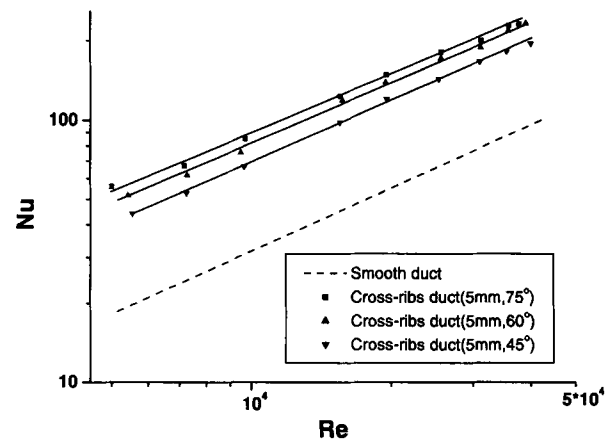
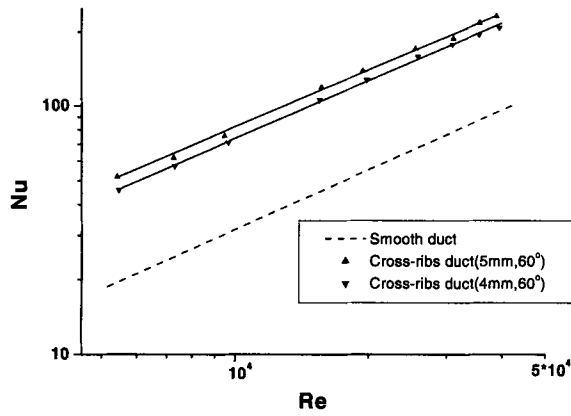
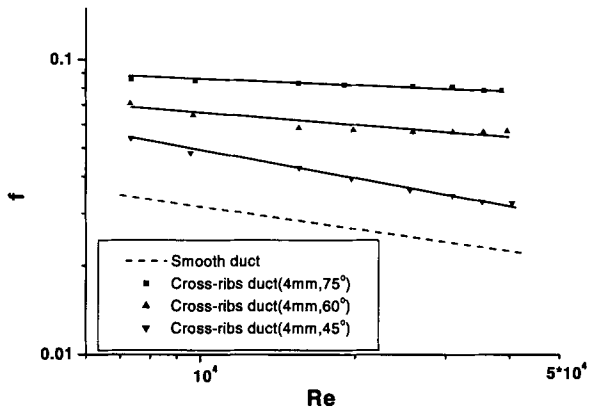
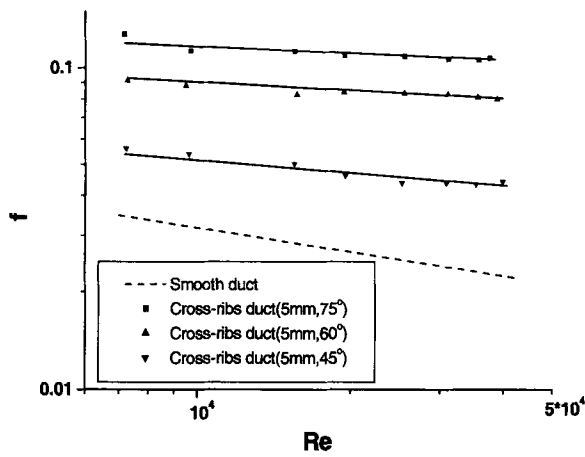
(f)  $f$  comparison between 4 mm and 5mm ribs

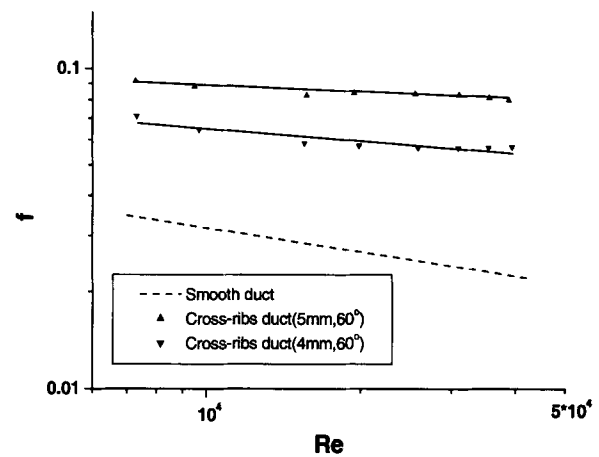
Fig. 9 The experimental results of group A-1

(a) Average  $Nu$  of 4 mm-rib duct(b) Average  $Nu$  of 5 mm-rib duct(c)  $Nu$  comparison between 4 mm and 5 mm ribs

(e) Duct friction factor of 5 mm-rib duct



(d) Duct friction factor of 4 mm-rib duct



(f) comparison between 4 mm and 5 mm

**Fig.10** The experimental results of group A-2

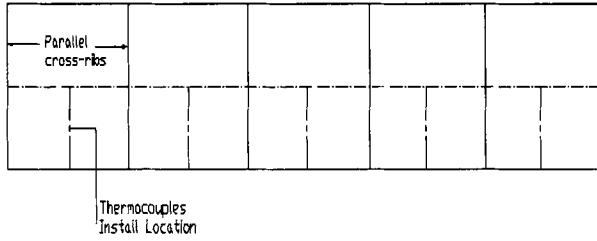


**Fig.11** The corresponding arrangements of two kinds of rib configuration

variety of constraints that may be employed. In this experiment, performance comparisons among the different types of cross-ribs and parallel ribs are made for two sets of constraints: (1) equal airflow rate, and (2) equal blowing (or pumping) power.

(1) Equal flow rate condition

For this constraint, we have:

$$(\dot{m})^* = \dot{m} \quad (6)$$

where the superscript \* stands for the compared duct, the quantity without \* for the reference duct.

For the same fluid, we have:

$$Re^* = Re_m \frac{D_m}{D_m^*} \quad (7)$$

Under the same temperature difference, the ratio of heat transfer rate is:

$$\frac{Q^*}{Q} = \frac{A^* \cdot Nu^*(Re_m^*)}{A \cdot Nu(Re_m)} \quad (8)$$

(2) Equal blowing power condition

For the same fluid and duct characteristic length we have

$$\left(\frac{\dot{m}}{\rho} \Delta p\right)^* = \left(\frac{\dot{m}}{\rho} \Delta p\right) \quad (9)$$

From Equation (5), the following two equations can be obtained:

$$(A_x f Re_m^3)^* = (A_x f Re_m^3) \quad (10)$$

This leads to:

$$Re^* = \sqrt[3]{\frac{(A_x f Re_m^3)^*}{(A_x f)^*}} \quad (11)$$

Thus under the same temperature difference, the ratio of heat transfer rate is:

$$\frac{Q^*}{Q} = \frac{A^* \cdot Nu^*(Re_m^*)}{A \cdot Nu(Re_m)} \quad (12)$$

Performance comparison was made for the case with rib height of 5 mm. In Figs.13,14, comparisons are made for two pairs of ducts: 45° cross-ribs vs 75° cross-ribs, and 45° cross-ribs vs 60° cross-ribs. The data are classified into two groups, in Group A-1 only one principal wall was roughened, while in Group A-2 two principal walls were both roughened. In Fig.15, comparisons are made for the case with 5 mm parallel ribs and 5 mm, 60° cross-ribs, two opposite walls were both heated and roughened.

#### Group A-1:

As shown in Fig.13, under equal flow rate condition, the heat transfer of 45° cross-ribs is 17% higher than 75° cross-ribs for  $Re < 10^4$ , but with the increase in  $Re$ , the enhancement of heat transfer rate decreases. The variation trend is the same for the comparison of 45° cross-ribs and 60° cross-ribs. The same variation pattern can be found for the comparison with identical pumping power. In sum, for the three angles of cross-ribs compared, the heat transfer rate of 45° cross-ribs is the highest, and that of 75° is the lowest with 60° cross-ribs being in between.

#### Group A-2:

As shown in Fig.14(a), under the condition of the equal flow rate, the heat transfer rate of 45° cross-ribs is 25% higher than 75° cross-ribs. As the  $Re$  increases, the ratio of heat transfer rate keeps constant. The heat transfer rate of 45° cross-ribs is 17% higher than 60° cross-ribs. With the increase in  $Re$ , the heat transfer enhancement of this case increases mildly.

Under the equal blowing power constraint (Fig.14(b)), when the flow rate is smaller than certain value, the heat transfer rate of 45° cross-ribs is a bit lower than 60° cross-ribs and 75° cross-ribs. Overall speaking, for the heat transfer rate, 45° cross-rib rank first, then comes 60° cross-ribs, and the rib of 75° is the worst, as that in the group A-1.

#### Group B:

From Fig.15(a), it can be seen that under the equal flow rate condition, the heat transfer rate of cross-ribs is 6% higher than parallel ribs for  $Re < 10^4$ . As the  $Re$  increases, the heat transfer enhancement ratio decreases a bit.

Under equal blowing power (Fig.15(b)), when the flow rate is smaller than certain value, the heat transfer rate of cross-ribs is a bit higher than that of parallel ribs, with the increase in  $Re$ , the ratio of the heat transfer rate

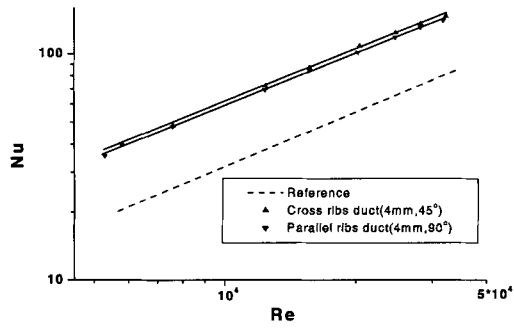
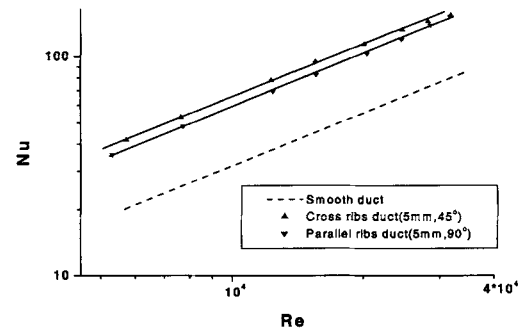
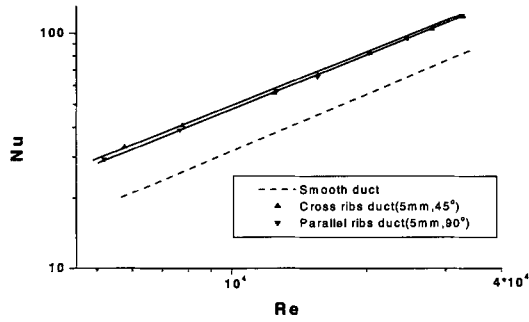
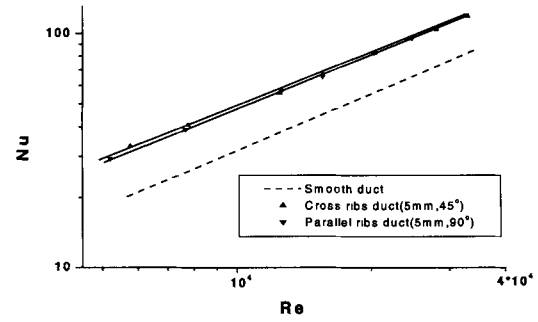
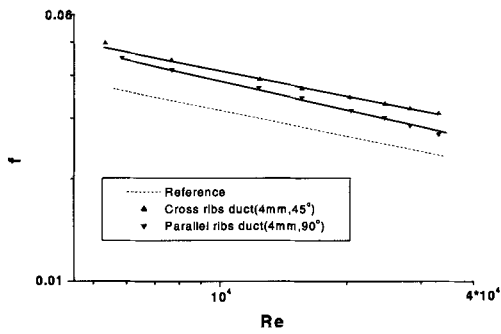
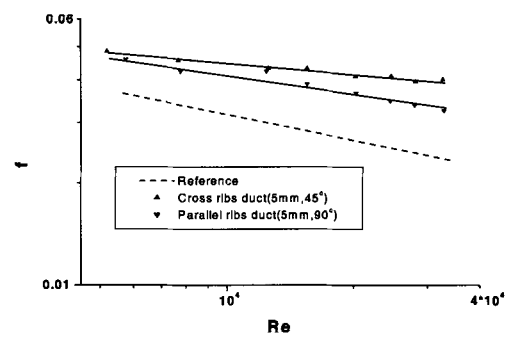
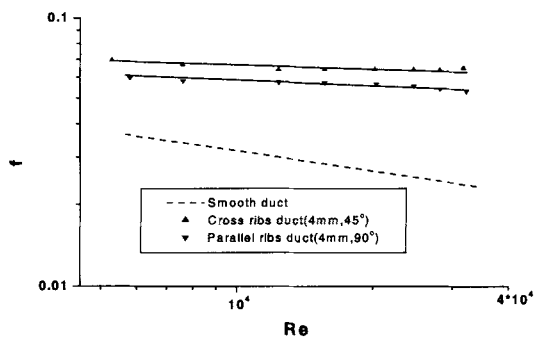
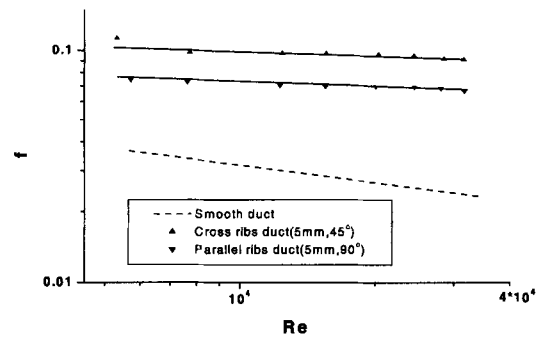
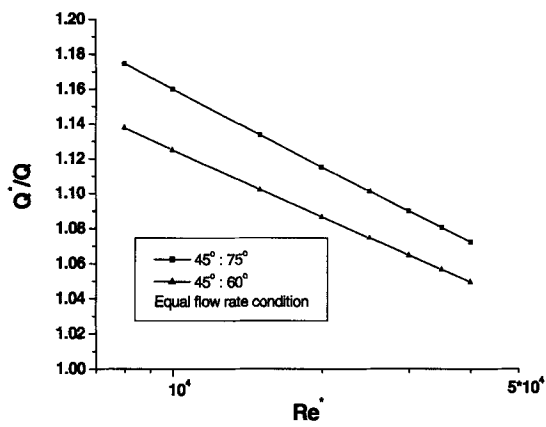
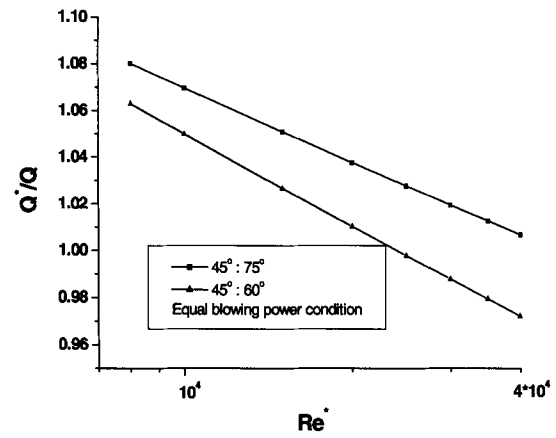
(a)  $Nu \sim Re$  (4 mm, two walls heat, one wall rib-roughened)(b)  $Nu \sim Re$  (5 mm, two walls heat, one wall rib-roughened)(c)  $Nu \sim Re$  (4 mm, both walls heat and roughened)(d)  $Nu \sim Re$  (5 mm, both walls heat and roughened)(e)  $f \sim Re$  (4 mm, two walls heat, one wall rib-roughened)(f)  $f \sim Re$  (5 mm, two walls heat, one wall rib-roughened)(g)  $f \sim Re$  (4 mm, both walls heat and roughened)(h)  $f \sim Re$  (5 mm, both walls heat and roughened)

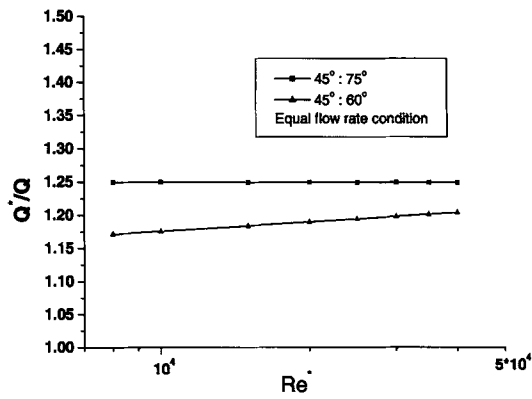
Fig.12 The experimental results of group B



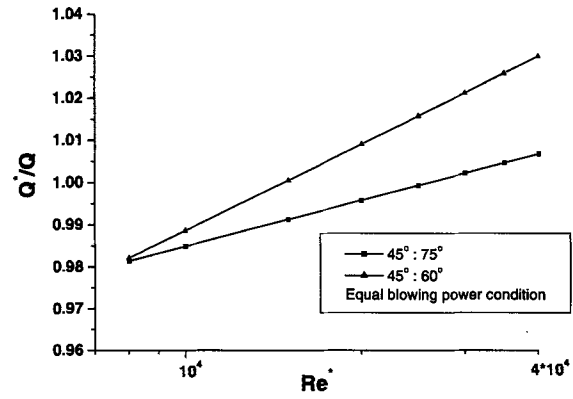
(a) Equal flow rate condition



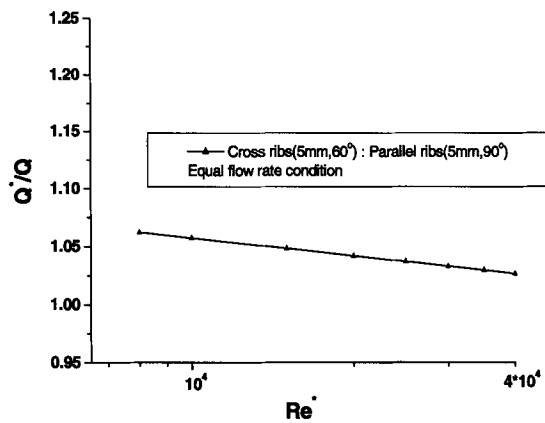
(b) Equal blowing power condition

**Fig.13** Comparison of the heat transfer performance for group A-1

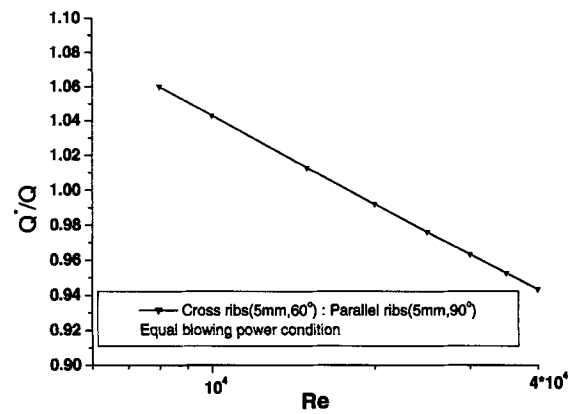
(a) Equal flow rate condition



(b) Equal blowing power condition

**Fig.14** Comparison of the heat transfer performance of group A-2

(a) Equal flow rate condition



(b) Equal blowing power condition

**Fig.15** Comparison of the heat transfer performance of group B

decrease greatly. In sum, for the heat transfer rate, in the low Reynolds number region, the cross rib has some advantage, while in the high Reynolds number region, the parallel ribs are a bit better than the cross-ribs.

## Discussion

It is generally believed that the rib-roughened surfaces can enhance convective heat transfer mainly because of the secondary flows induced by the small ribs installed on the smooth surfaces. Even though ribs also serve as fins and can increase the heat transfer area, both experimental measurement and numerical simulation show that compared with the secondary flow effect, these factors are insignificant<sup>[15,16]</sup>. In this regard, the surfaces with cross-ribs will certainly have higher heat transfer coefficient compared to the plain smooth surface because of the secondary flows induced by the ribs.

Compared with the parallel ribs, however, the cross ribs has a crossed region where the two opposite ribs meet each other. Each pair of two opposite ribs divides the surface into four regions, each of which is surrounded by two opposite ribs. In these angle regions the development of the vortices may be retarded, and developed vortices may interact with each other. Thus, the existence of the crossed region may result in some negative effect on heat transfer. At low Reynolds number, these interactions may not be significant, and the heat transfer may be enhanced in some extent. While at high Reynolds number, the interaction of the secondary flows may deteriorate the heat transfer. Our experimental findings are qualitatively agree with the results reported in [1], where it is found that the crossed oblique discrete ribs perform poorly compared with 90 degrees discrete ribs in the Reynolds number range from 10000 to 80000.

## Conclusion

The duct average turbulent heat transfer and friction factor in square channels with one or two principal walls roughened by cross-ribs have been investigated experimentally in the following parameter range: cross rib angles = 45°, 60°, 75°, relative rib height = 0.08, 0.10, Reynolds number =  $5 \times 10^3 \sim 4 \times 10^4$ . Correlations of  $Nu \sim Re$  and  $f \sim Re$  are obtained for 12 combinations. The major conclusions can be drawn as follows:

1. For the cross rib arrangements studied, the rib height and cross angle have positive effect on heat transfer; the larger the cross angles and the rib height, the higher the heat transfer coefficients. At the same time, the friction factor also increase accordingly.

2. Compared with the parallel rib configuration, the

cross-rib arrangement can enhance heat transfer when the Reynolds number is smaller than a certain value, with the increase of Reynolds number, the ratio of heat transfer rate of cross-ribs to parallel ribs decreases greatly. In the high Reynolds number region, the heat transfer performance of parallel ribs seems better than that of the cross ribs.

## Acknowledgements

The work described in this paper has been supported by a grant from the Research Grants Council of the Hong Kong Special Administrative Region, China (Project No. PolyU 5156/99E).

## References

- [1] Lau S C, McMillin R D, Han J C. Turbulent Heat Transfer and Friction in a Square Channel with Discrete Rib Turbulators. *Journal of Turbomachinery*, 1991, 113: 360–366
- [2] Han J C. Square Channels with Parallel, Crossed, and v-Shaped Angled Ribs. *Journal of Heat Transfer*, 1991, 113: 590–596
- [3] Liou T M, Hwang J J. Effect of Ridge Shapes on Turbulent Heat Transfer and Friction in a Rectangular Channel. *Int. J. Heat Mass Transfer*, 1993, 36: 931–940
- [4] Lorenz S, Mukomilow D, Leiner W. Distribution of Heat Transfer Coefficient in a Channel with Periodic Transverse Grooves. *Experimental Thermal and Fluid Science*, 1995, 3: 234–242
- [5] Hwashida M. Local Heat Transfer Coefficient Distribution on a Ribbed Surface. *J. Enhanced Heat Transfer*, 1996, 3: 187–200
- [6] Hwang J J, Liou T M. Heat Transfer Augmentation in a Rectangular Channel with Slit Rib-Turbulators on Two Opposite Walls. *Journal of Turbomachinery*, 1997, 119: 617–623
- [7] Saini R P, Saini J S. Heat Transfer Augmentation in a Rectangular Channel with Slit-Turbulators with Expended Metal Mesh as Roughness Element. *Int. J. Heat & Mass Transfer*, 1997, 40(4): 973–986
- [8] Chandra P R, Fontenot M L, Han J C. Effect of Rib Profiles on Turbulent Channel Flow Heat Transfer. *J. Thermophysics & Heat Transfer*, 1998, 12(1): 116–118
- [9] Leung C W, Chen S, Wong T T. Forced Convection and Pressure Drop in a Horizontal Triangular-Sectional Duct with v-Grooved Inner Surfaces. *Applied Energy*, 2000, 66: 199–211
- [10] Wang L B, Tao W Q, Wang Q W, et al. Experimental Study of Developing Turbulent Flow and Heat Transfer in Ribbed Convergent/Divergent Square Ducts. *Int. J. Heat Fluid Flow*, 2001, 22: 603–613
- [11] Fujii T. Overlooked Factors and Unsolved Problems in Experimental Research on Condensation Heat Transfer.

- Experimental Thermal and Fluid Science, 1992, 5: 652—663
- [12] Rose J W. Heat-Transfer Coefficient, Wilson Plots and Accuracy of Thermal Measurements. In: Compact Heat Exchangers, A Festschrift on the 60<sup>th</sup> birthday of Ramesh Shah, Edizioni ETS, Piza, Italy, 2002
- [13] Wang L B. Experimental and Numerical Study of Turbulent Fluid and Heat Transfer in Sectionally Complex and Twisted Duct: [PhD Thesis]. Xi'an: Xi'an Jiaotong University, 1996
- [14] Yang S M, Tao W Q. Heat Transfer. 3<sup>rd</sup> Ed.. Beijing: Higher Education Press, 1998
- [15] Han J C, Zhang P. Effect of Rib Angle Orientation on Local Mass Transfer Distribution in a Three-Pass Rib-Roughened Channel. ASME J Turbomachinery, 1991, 113: 123—130
- [16] Zhao C Y. The Study of Turbulent Flow and Heat Transfer in Two-Pass Channels and Rotating Cavities: [PhD Thesis]. Xi'an: School of Energy & Power Engineering, Xi'an Jiaotong University, 1996